On the Synthesis of Quinone-based BODIPY Hybrids: New Insights on Antitumor Activity and Mechanism of Action in Cancer Cells

On the Synthesis of Quinone-based BODIPY Hybrids: New Insights on Antitumor Activity and Mechanism of Action in Cancer Cells

Talita B. Gontijo,[a] Rossimiriam P. de Freitas,[a] Flavio S. Emery,[b] Leandro F. Pedrosa,[c] José B. Vieira Neto,[d] Bruno C. Cavalcanti,[d] Claudia Pessoa,[d,e] Aaron King,[f] Fabio de Moliner,[f] Marc Vendrell[f]* and Eufrânio N. da Silva Júnior[a]*

[a]Institute of Exact Sciences, Department of Chemistry, Federal University of Minas Gerais, Belo Horizonte, 31270-901, MG, Brazil. E-mail: eufranio@ufmg.br; Tel: +55 31 34095720; [b]Faculty of Pharmaceutical Sciences at Ribeirao Preto, University of São Paulo, CEP 14040-903, Ribeirão Preto, SP, Brazil; [c]Institute of Exact Sciences, Department of Chemistry, Fluminense Federal University, CEP 27213-145, Volta Redonda, RJ, Brazil; [d]Department of Physiology and Pharmacology, Federal University of Ceará, CEP 60180-900, Fortaleza, CE, Brazil; [e]Fiocruz-Ceará, CEP 60180-900, Fortaleza, CE, Brazil; [f]MRC/UoE Centre for Inflammation Research, The University of Edinburgh, EH16 4TJ Edinburgh, United Kingdom. E-mail: mvendrel@staffmail.ed.ac.uk; Tel: +44 (0)131 242 6685. Webpage: www.dynafluors.co.uk

Abstract: Fluorescent quinone-based BODIPY hybrids were synthesised and characterised by NMR analysis and mass spectrometry. We measured their cytotoxic activity against cancer and normal cell lines, performed mechanistic studies by lipid peroxidation and determination of reduced (GSH) and oxidized (GSSG) glutathione, and imaged their subcellular localisation by confocal microscopy. Cell imaging experiments indicated that nor-β-lapachone-based BODIPY derivatives might preferentially localise in the lysosomes of cancer cells. These results assert the potential of hybrid quinone-BODIPY derivatives as promising prototypes in the search of new potent lapachone antitumor drugs.

Keywords: Quinone; BODIPY; Lapachone; Cancer; Subcellular localization.

1. Introduction

Over the years, medicinal chemists have been improving several chemical strategies for the discovery of new drugs.[1] For example, enzymatic targets have been used in molecular docking studies for computational drug design to predict the chemical structure of potential inhibitors.[2] Looking for new directions, late stage functionalization of drug-like molecules arises as a modern and elegant strategy in drug discovery programs, as recently reviewed by Cernak and coworkers.[3] Another strategy stems from the inspiration of natural products. Compounds isolated from diverse natural sources can be used as starting points to generate novel structures with varied biological activities.[4] As discussed by Newman and Cragg,[5] natural products still have a major role in the design of new antitumor drugs.

The search for antitumor drugs is a big challenge with multiple questions.[6] Some of the key questions are associated to the mechanism of action of cytotoxic drugs and the subcellular organelles where drugs preferentially accumulate. These questions can be generally answered by bioimaging experiments[7] as well as *in vitro* biological assays.[8]

Lapachones are naturally occurring naphthoquinones and among the most studied quinones due their potent antitumor activity.[9] Lately, diverse lapachone derivatives have been reported as potent cytotoxic drugs against different cancer cell lines.[10] In this regard, advances in the synthesis of lapachones with potent antitumor activity have been accomplished via modification of the A- and C-rings,[11] with recent progress being achieved by da Silva Júnior,[12] Pinto,[13] Hong,[14] Ferreira,[15] Bonifazi,[16] among others[17] (Scheme 1A).

As studied by the Boothman group, the mechanism of action of most β-lapachones is related to the destruction of cancer cells with elevated levels of NAD(P)H:quinone oxidoreductase 1 (NQO1).[18,19,20] Recently, Ohayon and coworkers[21] have shed some light on the possibility that β-lapachones might act non-reversibly as inhibitors of deubiquitinases. The therapeutic effect of β-lapachones could be also related to the oxidation of ubiquitin specific peptidase 2 (USP2), as a likely downstream effect of reactive oxygen species (ROS) generation.

In this context, unraveling the mechanism of action of antitumor lapachone derivatives is a recurring challenge for the scientific community. In the last few years, our group has dedicated great efforts to prepare fluorescent lapachones by hybridization of the quinoidal moiety with fluorescent compounds, such as the benzothiadiazole structure (Scheme 1B).[22] Fluorescent lapachones allow us to answer critical questions related to their mechanism of pharmacological action, including subcellular localization studies in live cells.[23] Recently, our group has described the first fluorescent lapachone-BODIPY hybrid as well as biological studies, including cytotoxic activity in different cancer cell lines and cell imaging experiments (Scheme 1B).[24]

Herein, we have developed a new chemical platform to prepare new lapachone derivatives coupled to the fluorescent BODIPY core, which has excellent photophysical properties.[24b] Lapachones exhibit potent antitumor activity due to their ability to act on multiple targets, as we have recently demonstrated.[25] This family of quinoidal derivatives can be divided into α-lapachones (*para*-quinones) and β-lapachones (*ortho*-quinones). We have demonstrated that both α- and β-lapachones display cytotoxic activity in cancer cells.[26] In the present work, we have synthesized a small collection of α- and β-lapachone derivatives (Scheme 1C) and evaluated their cytotoxicity in human

cancer and non-cancerous cell lines. Furthermore, we have also prepared fluorescent BODIPY-lapachones to examine the subcellular localization of lapachone-based compounds in cancer cells and any derived effects in their cytotoxic activity.

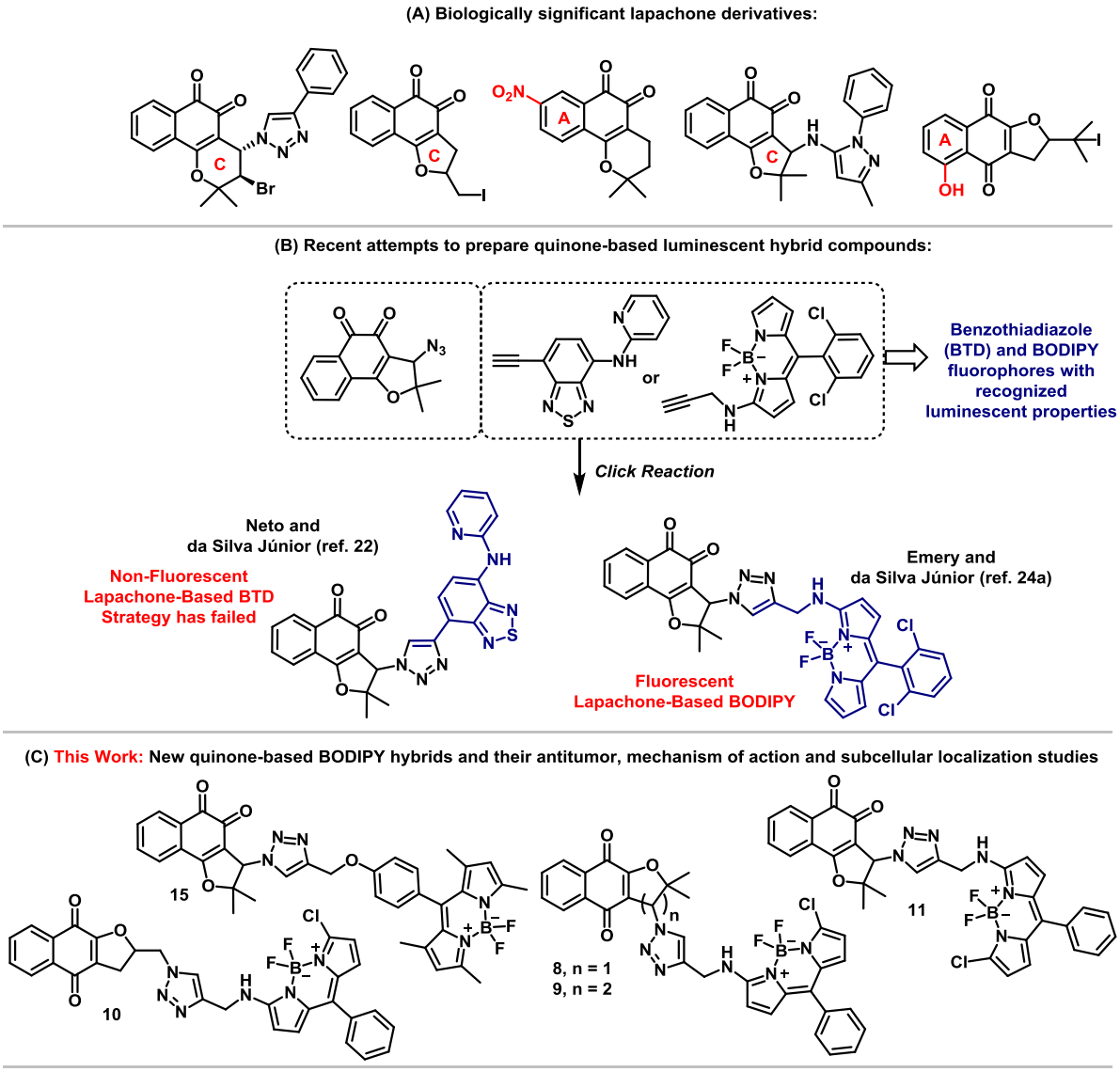

Scheme 1. Overview of lapachone derivatives and the design of quinone-based BODIPY hybrids.

2. Results and discussion

The synthesis of the quinone-based BODIPY hybrids **8-11** was accomplished by a convergent synthetic route,[24] using a classical copper(I)-catalyzed alkyne-azide cycloaddition (CuAAC) reaction.[27] We used an alkyne-containing BODIPY and azide-containing quinones to assemble fluorescent, hybrid quinoidal-BODIPY molecules. We started the preparation of quinone-containing BODIPYs by the synthesis of boron-dipyrromethene with a terminal alkyne for subsequent CuAAC reaction. There are numerous reports on synthetic approaches to generate BODIPY scaffold with bespoke spectral properties.[28] Among them, we used the methodology from the Dehaen group with minor modifications[30] for preparing compound **3**. With regards to the azides **4-7**, we initially prepared 3-azido-nor-α-lapachone (**4**) and 4-azido-α-lapachone (**5**) from lapachol. The methodology for the synthesis of **4** and **5** is well described in the literature.[31,32] Cyclic lapachones were obtained by insertion of bromine atoms and nucleophilic substitution with sodium azide to afford the respective clickable analogues **4** and **5**.

The synthesis of azides **6** and **7** was conducted following methodologies described by our group.[25,26,33] Compound **6** was prepared from C-allyl lawsone upon reaction with iodine to obtain the cyclized product, which underwent nucleophilic substitution with sodium azide. Finally, the last clickable derivative **7** was obtained from nor-lapachol, previously synthesized from lapachol, by the well-established Hooker oxidation method.[34] Nor-lapachol was transformed into the key intermediate 3-bromo-nor-β-lapachone, which was reacted with sodium azide to render 3-azide-nor-β-lapachone (**7**). Once the azido-quinones **4-7** and the alkyne BODIPY **3** were obtained,

we readily prepared a small collection of quinone-based BODIPY hybrids (**8-11**) in good yields (Scheme 2).

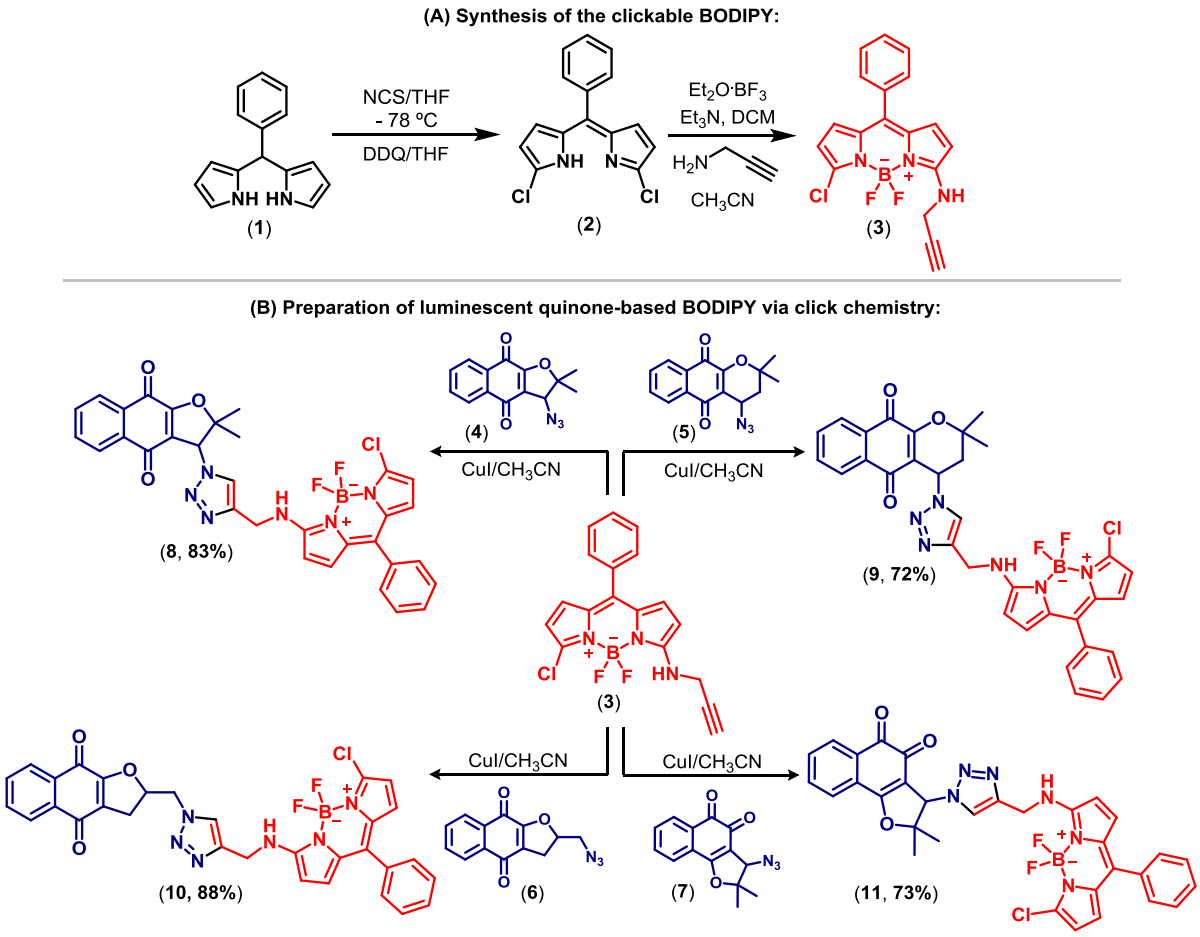

Scheme 2. Synthesis of quinone-based BODIPY hybrids **8-11**.

Lapachone-based BODIPYs **8-11** were evaluated for *in vitro* cytotoxicity using an MTT assay in five human cancer cell lines (i.e. PC3, SF295, MDA-MB435, SW620 and HCT-116) and two murine non-cancer (L929 and V79) cells. As previously reported,[35] compounds **8-11** were classified according to their cytotoxicity against cancer cells as highly active (IC_{50} < 2 μM), moderately active (2 μM < IC_{50} < 10 μM), or inactive (IC_{50} > 10 μM). As shown in Table 1, no active *para*-quinones (**8-10**) were

identified. We have reported α-lapachone derivatives with potent cytotoxicity against cancer cells prepared by C-ring modification and insertion of arylamino groups at positions C-3 (nor-α-lap) and C-4 (α-lap).[36] In fact, molecular hybridization[37] between α-lapachones and 1,2,3-triazole groups has been reported as an efficient strategy for antitumour compounds.[22] Herein, the same approach rendered hybrids compounds (**8-10**) that were not active against any the tested cancer cell lines, with IC_{50} values round 8 μM for all compounds.

On the other hand, compound **11** exhibited significant cytotoxicity against all human cancer cell lines with IC_{50} values in the low micromolar range (i.e. 0.3 to 0.9 μM, Table 1). This observation is in line with previous reports of *ortho*-quinones (i.e. β-lapachone) being more active than the corresponding *para*-quinones, such as α-lapachone.[38] Moreover, Abreu and collaborators[39] have shown that the radicals generated during the reduction of β-lapachones reduction confer more stability to reduced *ortho*-quinone derivatives when compared to their reduced *para*-isomers. As a result, *ortho*-quinones, such as the hybrid derivative **11**, might present better redox cycling ability, which is the ability of a molecule to undergo repeated reduction and oxidation, producing more free radicals than compounds **8-10** (*para*-quinones), which is in agreement with the absence of cytotoxicity determined for **8-10**.

Table 1. Cytotoxic activity expressed by IC_{50} (μM, 95% CI) of compounds **8-11** in cancer[a] and normal cells[b] after 72 h. Values obtained by nonlinear regression from three independent experiments and compared to the antitumor drug doxorubicin (DOXO).

Compd	PC3	SF295	MDA-MB435
8	> 8.10	> 8.10	> 8.10

9	> 7.83	> 7.83	> 7.83	
10	> 8.19	> 8.19	> 8.19	
11	0.38 (0.35-0.41)	0.28 (0.17-0.40)	0.81 (0.67-0.91)	
DOXO	0.05 (0.02-0.07)	0.45 (0.41-0.49)	0.94 (0.89-0.98)	
Compd	**SW620**	**HCT-116**	**L929**	**V79**
8	> 8.10	> 8.10	> 8.10	> 8.10
9	> 7.83	> 7.83	> 7.83	> 7.83
10	> 8.19	> 8.19	> 8.19	> 8.19
11	0.68 (0.60-0.75)	0.32 (0.25-0.38)	0.92 (0.75-1.00)	0.65 (0.51-0.72)
DOXO	0.29 (0.26-0.37)	0.21 (0.18-0.23)	0.22 (0.19-0.24)	0.25 (0.21-0.28)

[a]PC3 prostate carcinoma, SF295 glioblastoma, MDA-MB435 melanoma, and SW620 and HCT-116 colon carcinomas cell lines. [b]Chinese hamster V79 and mouse L929 cells.

The lapachone derivative **11** presented high activity in all the cancer cell lines evaluated, showing the strongest effect in human glioblastoma cells (SF295) with an IC_{50} value around 300 nM. This result represents an improvement in the potency of previously described lapachone-based BODIPY derivatives.[24] The results against non-tumor cells showed that **11** presented IC_{50} values in V79 and L929 cells in the range 0.92-0.65 µM. These results indicate that **11** was slightly less cytotoxic against non-tumor cells, with selectivity indexes (i.e. ratio of cytotoxicities between cancer and normal cells) around 3. Whereas further optimization of the lapachone structure would be needed to enhance these selectivity indexes, these values are in line with those of doxorubicin, a clinically used antitumor drug and one of the most potent and important antitumor quinones.

Quinones are highly redox active molecules leading to formation of reactive oxygen species (ROS), which cause oxidative stress by oxidising lipids, proteins and DNA.[40] Lipid peroxidation is a well-established mechanism of cellular damage, and it can be used as an intracellular indicator of oxidative stress. The measurement of malondialdehyde (MDA), which is one of the most abundant products from lipid peroxidation, is a highly sensitive assay to quantitatively evaluate the formation of lipid peroxides in cells. We determined the levels of MDA in three cancer cell lines (prostate, glioma and colon) and one non-tumor cell line (murine fibroblast) 24 h after exposure of compound **11**, and observed that the levels of MDA in all cancer cells as well as normal fibroblasts evaluated were significantly higher than in the controls (Figure 1). In addition, when comparing the equal concentrations of compound **11** between cell lines used in this current study, there is no more sensitive strain than another in relation to the extent of byproduct of lipid peroxidation, thiobarbituric acid reactive substances (TBARS) formation. Moreover, the pretreatment of the cells with *N*-acetylcysteine (NAC) showed a strong protective effect by preventing lipid peroxidation mainly by promoting GSH synthesis by NAC, and by its ROS scavenger ability[41] highlighting the prooxidant mechanism linked to cancer and non-cancer cells death. The role of ROS as an important colaborative factor in cell death was well correlated by variation of thiols content after tested compound exposure. Oxidative stress burden usually correlates with cellular thiol levels or vice versa cellular thiol/disulfide ratio is a well-accepted indicator of the redox state of a cell.[42] Naphthoquinones with higher redox potential showed stronger cytotoxicity, presumably because of stronger electrophilicity against thiols and because their GSH conjugates are more readily reduced to semiquinones which activate oxygen.[43] To determine whether oxidative stress induced by compound **11** is accompanied by changes in total glutathione, the reduced (GSH), oxidized glutathione

(GSSG) and GSH/GSSG ratio were measured. After 24 h exposure, compound **11** significantly reduced ($p<0.05$) the total content of glutathione of all cell cultures (Table 2) The decrease in total amount of glutathione after compound **11** exposure was accompanied by an increase in GSSG levels ($p<0.05$) in relation to non-treated cultures. Due to observed compound **11** exposure effects on both reduced and oxidized glutathione the ratio of GSH/GSSG was decreased. On the other hand, in all cultures pre-exposed to NAC before quinone treatment the level of total glutathione was kept nearly or slightly above at the control value.

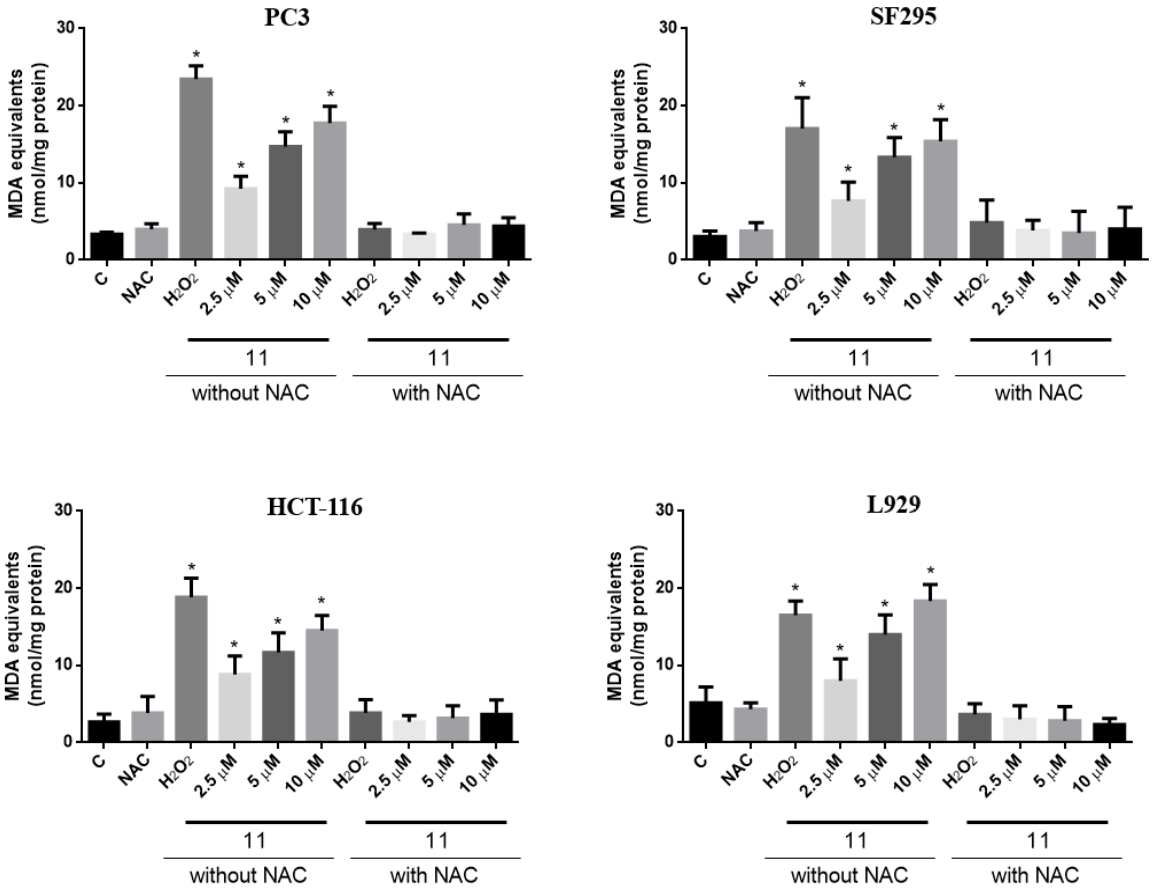

Figure 1. Determination of MDA levels (TBARS assay) in human cancer cells (PC3, SF295 and HCT-116) and in non-cancer mouse fibroblasts (L929) after 24 h-incubation with compound **11** or 10 μM H_2O_2 (positive control) in the presence or absence of NAC

(5 mM). *p < 0.05 as compared to control by ANOVA followed by Tukey's test. Values as means ± s.e.m. for three independent experiments in triplicate.

However, the neutralization of ROS by pretreatment with NAC suggests that an alternative mechanism different from ROS generation might be involved in the cytotoxic effect of compound **11**, as stated in Table 3, in co-treated (GSH-OEt + naphthoquinones) cancer and non-cancer cells, GSH-OEt only reduced the sensitivity of compound **11** exposure but not abrogated it, which pointed that another mechanism differently of ROS generation capacity may be involved in its cytotoxic effects. Quinonoid compounds can potentially damage multiple macromolecules in cells, such as DNA, resulting in single or double strand breaks or the formation of oxidative nucleobases such as 8-oxo-7,8-dihydroguanine, thymine and uracil glycol.[44] In order to assess this possibility, we performed comet assays, which are consistent with the reported DNA damage potential attributed to quinonoid molecules.[45] Compound **11** caused DNA strand breaks after 24 h exposure in all three cancer cell lines as well as in murine fibroblasts. In relation to the antioxidant potential of NAC, it is known that NAC can regulate of oxidative stress related gene expression, having an antagonistic effect on oxidative injuries.[47] However, as shown in Figure 2, NAC pretreatment did not prevent DNA damage but only resulted in slightly lower levels of fragmented DNA. Altogether, these results suggest that the high cytotoxicity of compound **11** is not exclusively limited to the generation of ROS generation. The results of ongoing studies in our laboratories will be reported in due course.

Table 2. Effects of compound **11** on intracellular thiols after 24 h with or without NAC pretreatment.

			Intracellular thiols (µg/mg protein)			
Cell line	**Treatment**	**Concentration**	**Total**	**GSH**	**GSSG**	**GSH/GSSG**
PC3	Control[a]	0.1% DMSO	4.23 ± 0.75	3.04 ± 0.51	1.11 ± 0.12	2.69 ± 0.21
	NAC	5 mM	4.74 ± 0.50	3.53 ± 0.33	1.18 ± 0.21	2.87 ± 0.55
	11	5 µM	3.53 ± 0.81*	1.35 ± 0.10*	2.16 ± 0.15*	0.37 ± 0.11*
	11 plus NAC[b]	5 µM	4.26 ± 0.55	3.13 ± 0.22	1.07 ± 0.15	2.88 ± 0.33
SF295	Control	0.1% DMSO	4.51 ± 0.83	3.16 ± 0.21	1.31 ± 0.55	2.34 ± 0.56
	NAC	5 mM	4.86 ± 0.71	3.81± 0.55	1.02 ± 0.10	3.61 ± 0.81
	11	5 µM	3.44 ± 0.10*	1.31 ± 0.16*	2.09± 0.21*	0.39 ± 0.20*
	11 plus NAC	5 µM	4.72 ± 0.22	3.47 ± 0.55	1.21 ± 0.10	2.82 ± 0.10
HCT-116	Control	0.1% DMSO	5.02 ± 0.91	3.74 ± 0.55	1.19 ± 0.37	3.09 ± 0.33
	NAC	5 mM	5.38 ± 0.45	4.09 ± 0.61	1.23 ± 0.33	3.26 ± 0.21
	11	5 µM	3.81 ± 0.56*	1.78 ± 0.25*	2.01 ± 0.22*	0.56 ± 0.10*
	11 plus NAC	5 µM	5.12 ± 0.11	3.71 ± 0.25	1.38 ± 0.33	2.63 ± 0.22
L929	Control	0.1% DMSO	4.87 ± 0.25	3.76 ± 0.51	1.05 ± 0.33	3.55 ± 0.51
	NAC	5 mM	5.43 ± 0.81	3.89 ± 0.75	1.52 ± 0.10	2.52 ± 0.33
	11	5 µM	3.50 ± 0.15*	1.15 ± 0.21*	2.27 ± 0.33*	0.33 ± 0.10*
	11 plus NAC	5 µM	5.21 ± 0.33	3.89 ± 0.21	1.24 ± 0.25	3.08 ± 0.50

[a] Negative controls treated with vehicle (0.1% DMSO); [b] cells were pretreated for 24 h with NAC (5 mM); *$p < 0.05$ as compared to control by ANOVA followed by Tukey's test. Values as means ± s.e.m. for three independent experiments in triplicate.

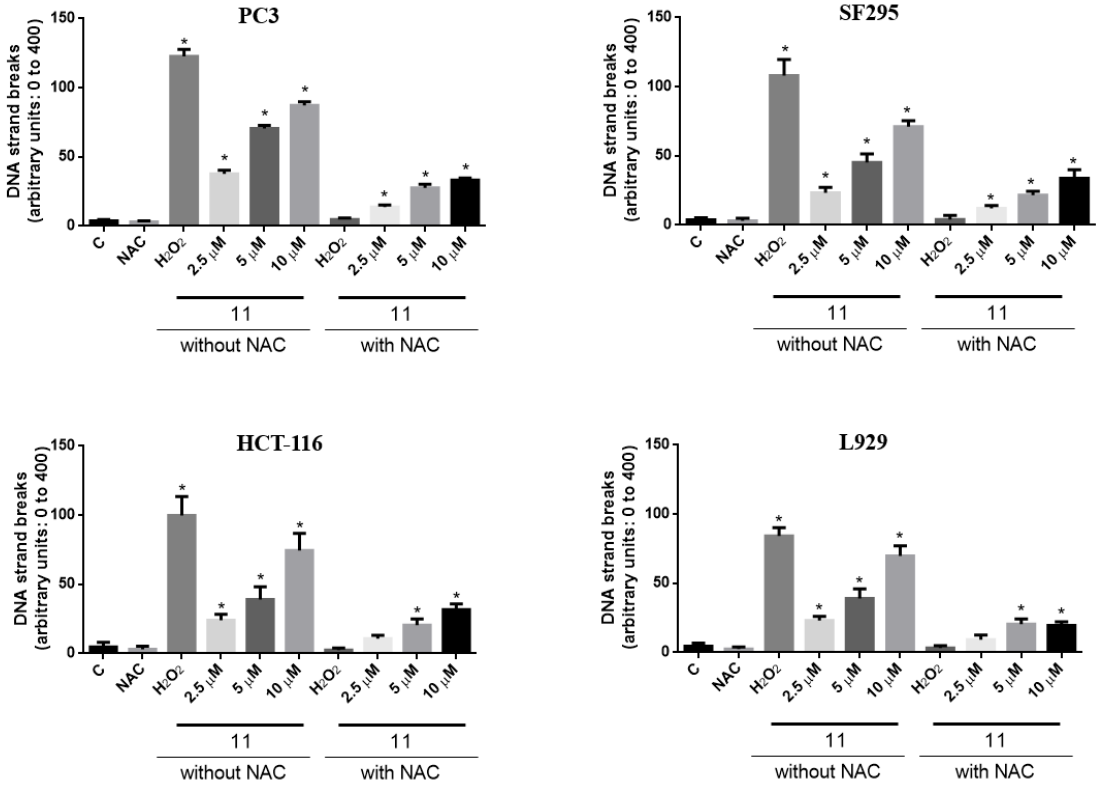

Figure 2. Effects of compound **11** on DNA strand breaks index after 24 h of exposure using alkaline comet assay exposure in the presence or absence of NAC (5 mM). *p < 0.05 as compared to control by ANOVA followed by Tukey's test. Data are presented as mean values ± SEMs for three independent experiments in triplicate.

Table 3. IC_{50} values (μM) for compounds **8-11** after 24 h of exposure in different cells in the presence or absence of reduced GSH.

Compound	GSH-OEt	PC3	SF295	HCT-116	L929
	+	> 40	> 40	> 40	> 40
8	-	> 40	> 40	> 40	> 40
	+	> 40	> 40	> 40	> 40
9	-	> 40	> 40	> 40	> 40
	+	> 40	> 40	> 40	> 40
10	-	> 40	> 40	> 40	> 40
	+	> 40	> 40	> 40	> 40

11	-	4.47 ± 0.73	1.96 ± 0.21	5.28 ± 0.55	5.91 ± 0.10
	+	15.83 ± 1.15	9.81 ± 0.10	14.25 ± 2.10	12.41 ± 1.75

[a] Cell-permeable ethyl ester analogue of reduced GSH (15 mM).

Finally, in order to analyse the subcellular localization studies of the lapachone-BODIPY hybrid **11**, we measured its photophysical properties. However, compound **11** presents a very low fluorescence quantum yield, which limits its capabilities for fluorescence cell imaging (Table 4 and Figures S16 and S17 in ESI). As reported for other BODIPY dyes,[47b] the amino group in the position **5** of the BODIPY core can cause significant quenching of the fluorophore via photoinduced electron transfer (PeT), making it unsuitable for imaging studies. Whereas the quenching effect is highly pronounced in compound **11**, the extent of PeT quenching is dependent on the structure of the quinone-based BODIPY core and the amino substituents. In view of these results, we synthesized the BODIPY-alkyne **14** as described in the literature and conjugated it to the quinone **7** by CuAAC reaction to render the hybrid BODIPY-quinone **15**.[48,49] We measured the photophysical properties of compound **15**, and as expected, determined its excitation and emission maxima in the green visible range, with high extinction coefficients and fluorescence quantum yields (Table 4 and Figure S1 in ESI), being a suitable fluorescent probe for live-cell imaging.

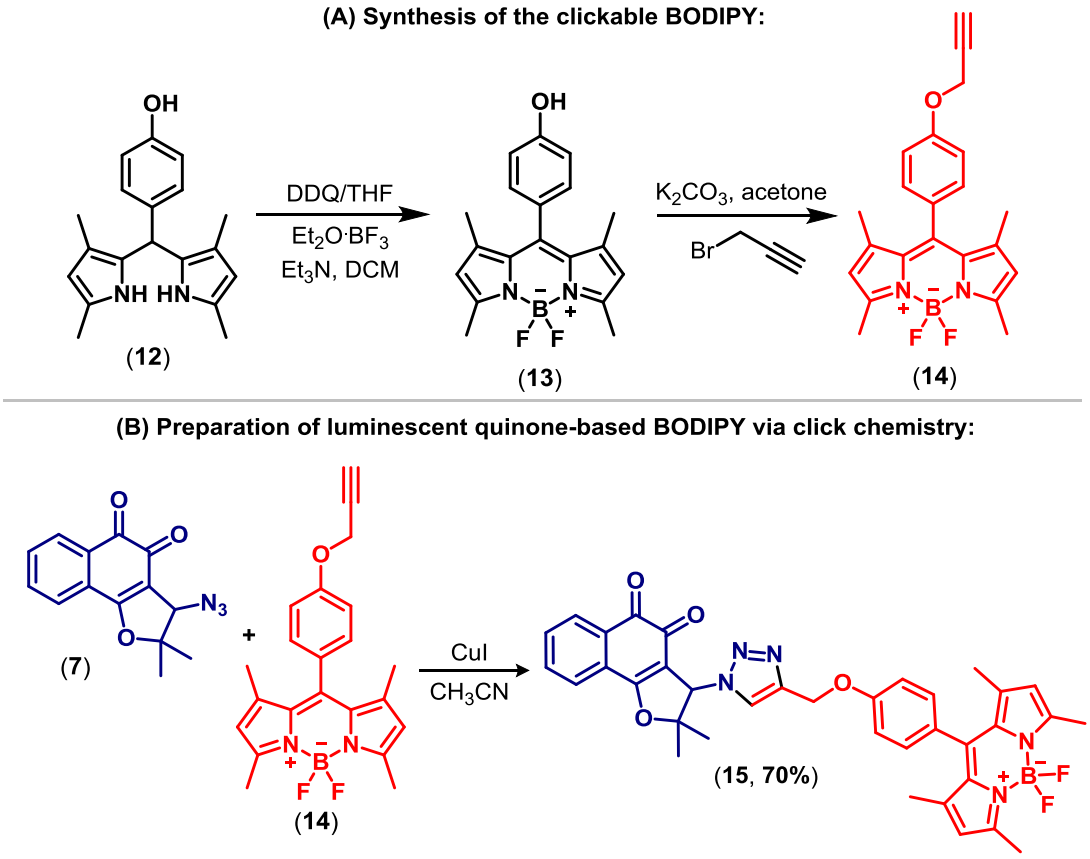

Scheme 3. Synthesis of the quinone-based BODIPY derivative **15**.

With compound **15** in hands, we tested its cytotoxicity in the same five cancer cell and non-cancer cell lines. Compound **15** displayed antiproliferative effects only in PC3 prostate and HCT-116 colon cell lines with IC_{50} values equal to 2.39 (2.14-2.65) and 2.85 (2.65-3.07) µM, respectively. For cancer cells (SF295, MDA-MB435 and SW620) and normal cells (L929 and V79) IC_{50} values were determined to be > 7.72 µM. Given the differences in cytotoxicity, we assessed the subcellular localization of compound **15** in PC3 cancer cells. Fluorescence confocal microscopy experiments revealed the preferential accumulation of **15** in the subcellular lysosomal compartments, showing strong co-localization with commercially available LysoTracker Red but not with MitoTracker Red dyes (Figure 3). Under these conditions, compound **11** was not

detectable under the fluorescence microscope due to its low quantum yield (Figure S18 in ESI).

Table 4. Photophysical data for compounds **11** and **15**.

Compound	$\lambda_{abs.}$(nm)	$\lambda_{abs.}$(nm)	ε ($M^{-1}cm^{-1}$)	QY[a]
11	495	530	30,300	0.03
15	498	511	68,800	0.82

[a] Determined as relative to fluorescein in basic EtOH (QY: 0.97).[49b]

Mefloquine, a known antimalarial and antitumoral molecule, has been reported to accumulate in the subcellular lysosomes of acute myeloid leukemia cells, where it exhibits high cytotoxicity due to lysosomal disruption.[50] This observation led us to evaluate the compound **15** in 2 leukemia cancer cell lines (HL-60 and Jurkat cells). Notably, **15** presented high activity in these cell lines with IC_{50} values in the low micromolar range [for HL-60 cells, IC_{50} = 0.92 (0.90-1.05) and for Jurkat cells, IC_{50} = 0.94 (0.86-0.98) μM]. Furthermore, because compound **15** showed very low cytotoxicity in non-cancer cells (i.e. L929 and V79), its selectivity index was over 8.5 (i.e. ~7-fold higher than compound **11**). Finally, we also assessed the effect of compound **15** on intracellular thiols in HL-60 and Jurkat cancer cell lines (Table 5). Remarkably, a weaker protective effect was observed for cells pretreated with NAC, suggesting a different mechanism of action between both lapachone-BODIPY hybrids. The ROS-independent cytotoxic effect of compound **15** is in line with the subcellular localization studies and its potential activity in lysosomal disruption of leukemia cancer cells.

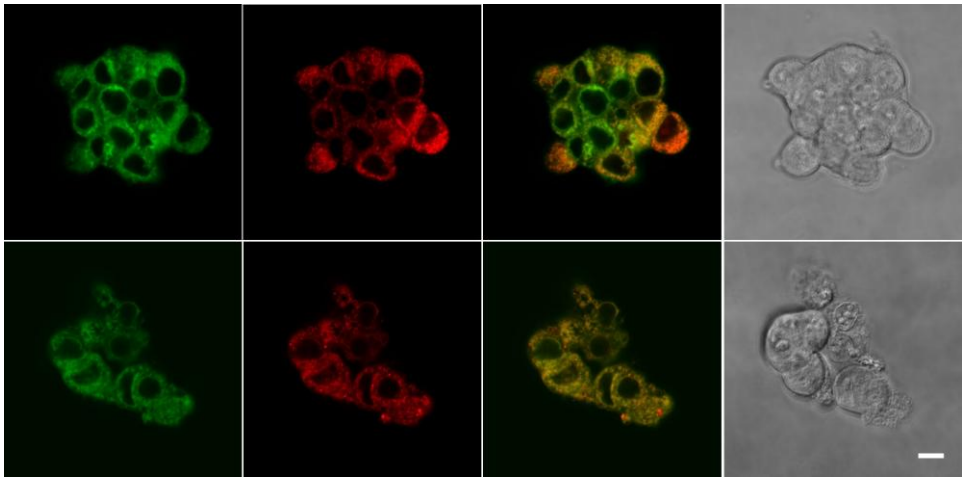

Figure 3. Fluorescence confocal microscopy of PC3 cells upon incubation with compound **15** as well as Mitotracker Red (*top panel*) and LysoTracker Red (*bottom panel*). Images arranged from left to right as: green fluorescence (**15**), red fluorescence (MitoTracker/LysoTracker), merged green/red channels and brightfield images. Scale bar: 10 μm.

Table 5. Effects of compound **15** on intracellular thiols after 24 h of cell exposure with or without NAC pretreatment.

			Intracelular thiols (μg/mg protein)			
Cell line	**Treatment**	**Concentration**	**Total**	**GSH**	**GSSG**	**GSH/GSSG**
HL-60	Control[a]	0.1% DMSO	3.61 ± 0.22	3.01 ± 0.11	0.66 ± 0.17	4.53 ± 0.55
	NAC[b]	5 mM	3.85 ± 0.81	3.03 ± 0.25	0.75 ± 0.90	4.02 ± 0.61
	15	5 μM	3.01 ± 0.44*	0.72 ± 0.20*	2.18 ± 0.10*	0.31 ± 0.05*
	15 plus NAC[c]	5 μM	2.83 ± 0.71*	1.19 ± 0.10*	1.47 ± 0.33*	0.76 ± 0.10*
Jurkat	Control[a]	0.1% DMSO	3.87 ± 0.55	3.02 ± 0.21	0.78 ± 0.33	3.81 ± 0.22
	NAC[b]	5 mM	4.13 ± 0.25	3.25 ± 0.17	0.81 ± 0.55	3.97 ± 1.17
	15	5 μM	3.28 ± 0.60*	0.60 ± 0.33*	2.57 ± 0.10*	0.21 ± 0.11*
	15 plus NAC[c]	5 μM	3.11 ± 0.05*	1.58 ± 0.55*	1.44 ± 0.51*	1.08 ± 0.33*

[a] Negative controls treated with vehicle (0.1% DMSO); [b] cells were pretreated for 24 h with NAC (5 mM); *p < 0.05 as compared to control by ANOVA followed by Tukey's test. Values as means ± s.e.m. for three independent experiments in triplicate.

3. Conclusions

We have synthesized and characterized a small collection of novel quinone-based BODIPY hybrids of the natural products lapachol and lawsone. All compounds were evaluated in cancerous and non-cancerous cell lines, and we identified two nor-β-lapachone hybrids (**11** and **15**) with potent cytotoxic activity. Mechanistic studies for both compounds suggest that the action of compound **11** may be related to the generation of reactive oxygen species whereas the fluorescent lapachone **15** may exert its cytotoxic action in subcellular lysosomal organelles. This study provides new structure-activity relationships in the preparation of biologically active lapachone derivatives as well as new insights in the potential mechanism of action for their cytotoxic activity.

4. Experimental Section

4.1. Chemistry

Melting points were obtained on Thomas Hoover and are uncorrected. Analytical grade solvents were used. Column chromatography was performed on silica gel (SilicaFlash G60 UltraPure 60-200 µm, 60 Å). ^{1}H and ^{13}C NMR were recorded at room temperature using a Bruker AVANCE DRX400, in the solvents indicated, with TMS as

internal reference. Chemical shifts (δ) are given in ppm. Electron-impact mass spectra (70 eV) were obtained using a VG Autospec apparatus (Micromass, Manchester, UK). Absorption spectra were obtained on a Varian Cary 100 spectrophotometer at room temperature in the solvents described above. Fluorescence spectra were obtained on a Varian Cary Eclipse spectrofluorimeter with a xenon arc lamp as the light source while using an excitation wavelength (λ_{exc}) corresponding to a higher absorption band. In all experiments, a quartz cuvette was employed with a 1 cm optical path length. Azide derivatives **4-7** and BODIPY **14** were synthesized as previously reported in the literature.[25,26,30-33] Structures of the novel compounds **3**, **8-11** and **15** were determined by ^{1}H and ^{13}C NMR. Electrospray ionization mass spectra were also obtained to confirm compound identities.

Procedure for the synthesis of BODIPY 3. To a solution of dichlorinated BODIPY (215 mg, 0.639 mmol) in acetonitrile (15 mL) under stirring at room temperature, propargylamine (102 µL, 1.6 mmol, 2.5 eq) was added. After 1 hour under stirring at room temperature TLC control showed full conversion of the starting material. Solvent was evaporated under reduced pressure and, after purification via silica column chromatography (C_6H_{14}/DCM, 3:2-1:3), the desired product **3** (201 mg, 0.56 mmol, 89% yield) was obtained. ^{1}H NMR (400 MHz, $CDCl_3$) δ: 7.49-7.43 (m, 5H), 6.93 (d, 1H, J = 4 Hz), 6.49 (br, 1H), 6.39 (d, 1H, J = 4 Hz), 6.28 (d, 1H, J = 4 Hz), 6.21 (d, 1H, J = 4 Hz), 4.17 (dd, 2H, J = 2.4 and 3.6 Hz), 2.38 (t, 1H, J = 2.4 Hz). ^{13}C NMR (100 MHz, $CDCl_3$) δ: 169.3, 135.9, 133.7, 133.2, 132.0, 131.2, 130.3, 129.5, 128.3, 121.6, 113.2, 110.9, 78.8, 34.1. EI/MS (*m/z*) $[M+H]^+$: 356.0. Calcd for $[C_{18}H_{14}BClF_2N_3]^+$: 356.0.

General procedure to prepare quinone-based BODIPY hybrids 8-11 and 15. In a round bottom flask, the respective azide derivatives (0.5 mmol), alkyne BODIPYs (0.6 mmol), and 10 mL of CH_3CN were added. The reaction mixture was stirred until complete solubilization of the reagents after which, CuI (10% per mole) was added. The system was kept under inert atmosphere (Ar) until complete consumption of BODIPY and monitored by TLC until its completion. The solvent from the crude was evaporated under reduced pressure and it was purified by column chromatography on silica-gel, using eluents with an increasing polarity gradient mixture of hexane and ethyl acetate.

Nor-α-lapachone-based BODIPY (8). Compound **8** was obtained as a brown solid after 18 h of reaction (258 mg, 83% yield); mp 173-175 °C. ^{1}H NMR (400 MHz, $CDCl_3$) δ: 8.16-8.14 (m, 1H), 8.05-8.03 (m, 1H), 7.75-7.73 (m, 2H), 7.59 (s, 1H), 7.48-7.44 (m, 5H), 6.86 (d, 1H, J = 4.8 Hz), 6.82 (sl, 1H), 6.35 (d, 1H, J = 3.8 Hz), 6.29 (d, 1H, J = 4.8 Hz), 6.18 (d, 1H, J = 3.8 Hz), 6.00 (s, 1H), 4.73 (d, 2H, J = 6.1 Hz), 1.74 (s, 3H), 1.16 (s, 3H). ^{13}C NMR (100 MHz, $CDCl_3$) δ: 180.9, 179.8, 177.8, 144.6, 135.9, 134.8, 135.9, 134.8, 133.6, 133.5, 131.9, 131.7, 130.5, 130.3, 129.3, 128.2, 127.2, 126.8, 126.5, 121.9, 121.1, 118.1, 94.3, 67.8, 40.4, 27.5, 21.0. EI/HRMS (*m/z*) $[M+Na]^+$: 647.1551. Calcd for $[C_{32}H_{24}BClF_2N_6O_3Na]^+$: 647.1557.

α-Lapachone-based BODIPY (9). Compound **9** was obtained as a brown solid after 18 h of reaction (229 mg, 72% yield); mp 171-173 °C. ^{1}H NMR (400 MHz, $CDCl_3$) δ: 8.12-8.10 (m, 1H), 7.95-7.93 (m, 1H), 7.69-7.67 (m, 3H), 7.47-7.42 (m, 5H), 6.87 (d,

1H, *J* = 4.4 Hz), 6.81 (sl, 1H), 6.35-6.32 (m, 2H), 6.17 (d, 1H, *J* = 3.6 Hz), 5.78 (t, 1H, *J* = 6.6 Hz), 4.74 (d, 2H, *J* = 6 Hz), 2.72 (dd, 1H, *J* = 14.6 and 6.8 Hz), 2.40 (dd, 1H, *J* = 14.6 and 6.8 Hz), 1.50 (s, 3H), 1.35 (s, 3H). ^{13}C NMR (100 MHz, $CDCl_3$) *δ*: 182.8, 179.3, 161.9, 156.2, 143.8, 135.9, 134.5, 133.7, 133.5, 132.7, 131.9, 131.8, 131.1, 131.3, 129.4, 128.3, 126.7, 126.4, 122.3, 120.9, 115.1, 112.9, 111.2, 79.3, 50.2, 40.5, 39.3, 26.9, 26.2. EI/HRMS (*m/z*) $[M+Na]^+$: 661.1704. Calcd for $[C_{33}H_{26}BClF_2N_6O_3Na]^+$: 661.1714.

Nor-α-lapachone-based BODIPY derivative (10). Compound **10** was obtained as a brown solid after 18 h of reaction (268 mg, 88% yield); mp 165-168 °C. ^{1}H NMR (400 MHz, $CDCl_3$) *δ*: 7.94 (d, 1H, *J* = 7.6 Hz), 7.91 (d, 1H, *J* = 7.6 Hz), 7.84 (s, 1H), 7.61 (t, 1H, *J* = 7.6 Hz), 7.55 (t, 1H, *J* = 7.6 Hz), 7.48-7.45 (m, 5H), 7.09 (sl, 1H), 6.85 (d, 1H, *J* = 4,8 Hz), 6.41 (d, 1H, *J* = 4.8 Hz), 6.33 (d, 1H, *J* = 4 Hz), 6.16 (d, 1H, *J* = 4.0 Hz), 5.40 (m, 1H), 4.82 (d, 2H, *J* = 5.2 Hz), 4.78 (d, 2H, *J* = 6.4 Hz), 3.41-3.34 (m, 1H), 3.04-2.97 (m, 1H). ^{13}C NMR (100 MHz, $CDCl_3$) *δ*: 181.7, 177.3, 161.9, 159.1, 144.7, 135.9, 134.2, 133.7, 133.4, 133.1, 132.6, 132.2, 131.9, 131.3, 130.3, 129.8, 129.3, 128.3, 126.2, 125.2, 124.2, 123.7, 120.4, 112.8, 111.4, 83.2, 53.0, 40.0, 30.2. EI/HRMS (*m/z*) $[M+Na]^+$: 633.1386. Calcd for $[C_{31}H_{22}BClF_2N_6O_3Na]^+$: 633.1401.

Nor-β-lapachone-based BODIPY (11). Compound **11** was obtained as a brown solid after 48 h of reaction (227 mg, 73% yield); mp 190-193 °C. ^{1}H NMR (400 MHz, $CDCl_3$) *δ*: 7.96 (d, 1H, *J* = 7.2 Hz), 7.83-7.79 (m, 2H), 7.73 (t, 1H, *J* = 8.9 Hz), 7.65 (t, 1H, *J* = 7.8 Hz), 7.46-7.42 (m, 5H), 6.89 (sl, 1H), 6.84 (d, 1H, *J* = 4 Hz), 6.34 (sl, 2H),

6.14 (sl, 1H), 6.00 (sl, 1H), 4.74 (d, 2H, J = 4.4 Hz), 1.77 (s, 3H), 1.17 (s, 3H). ^{13}C NMR (100 MHz, $CDCl_3$) δ: 180.2, 174.9, 171.4, 161.8, 144.3, 136.0, 134.6, 133.7, 133.2, 132.4, 131.9, 131.6, 130.3, 120.8, 129.3, 128.3, 126.8, 125.6, 122.3, 120.5, 112.8, 111.4, 111.4, 95.9, 67.1, 40.4, 27.7, 21.2. EI/HRMS (*m/z*) $[M+Na]^+$: 647.1521. Calcd for $[C_{32}H_{24}BClF_2N_6O_3Na]^+$: 647.1557.

Fluorescent nor-β-lapachone-based BODIPY (15). Compound **15** was obtained as a red solid after 48 h of reaction (226 mg, 70% yield); mp 176-179 °C. ^{1}H NMR (400 MHz, $CDCl_3$) δ: 8.21 (d, 1H, J = 7.2 Hz), 7.83 (t, 1H, J = 7.2 Hz), 7.79-7.73 (m, 2H), 7.64 (s, 1H), 7.18 (d, 2H, J = 8.0 Hz), 7.09 (d, 2H, J = 8.0 Hz), 6.03 (s, 1H), 5.98 (s, 2H), 5.24 (d, 2H, J = 4.0 Hz), 2.56 (s, 6H), 1.80 (s, 3H), 1.41 (s, 6H), 1.22 (s, 3H). ^{13}C NMR (100 MHz, $CDCl_3$) δ: 180.1, 174.6, 171.4, 158.9, 155.5, 143.9, 143.2, 141.7, 135.0, 133.6, 131.9, 131.7, 130.2, 129.4, 127.9, 126.7, 125.7, 122.5, 121.3, 115.6, 111.2, 96.0, 67.2, 62.3, 27.8, 21.3, 14.6. EI/HRMS (*m/z*) $[M+Na]^+$: 670.2401. Calcd for $[C_{36}H_{32}BF_2N_5O_4Na]^+$: 670.2413.

4.2 Biological Data

Inhibition of cell proliferation – MTT tests. Cell growth was quantified by the ability of living cells to reduce the yellow dye MTT to a purple formazan product. Cytotoxicity was checked on different human cancer cell lines (HL-60 and Jurkat leukemias, PC3 prostate carcinoma, SF295 glioblastoma, MDA-MB435 melanoma, SW620 and HCT-116 colon carcinomas cell lines), and two non-cancer murine fibroblasts (Chinese hamster V79 and mouse L929 cells). All cancer cells were obtained from the National

Cancer Institute in Bethesda, MD, USA. The V79 cells were kindly provided by Dr. Henriques JAP (Federal University of Rio Grande do Sul, Porto Alegre, Brazil), and L929 cells were purchased from Rio de Janeiro Cell Bank (BCRJ, Rio de Janeiro, Brazil). For the experiments, cells were plated in 96-well plates (0.7×10^5 to 0.3×10^6 cells/ well for cancer cells and 0.5×10^5 cells/well for murine fibroblasts), and tested compounds, dissolved in DMSO (0.1%), was then added to each well, followed by incubation for 24 h at concentrantions ranging from 0.04 to 40.92 μM or 72 h at concentrantions ranging from 0.04 to 8.19 μM. In some experiments, the contribution of ROS to the cytotoxicity of tested quinones was assessed by cells co-treated with GSH-OEt (15 mM). Our preliminary experiments showed that the ethyl ester of GSH was not cytotoxic and provided a more efficient protection than GSH at the same concentration (15 mM). In fact, GSH is not readily transported into most cells. Thus, in the MTT experiments, we used GSH ethyl ester, which is more lipophilic, readily taken up by cells and hydrolyzed to GSH by cellular nonspecific esterases.[51] Afterward, the plates were centrifuged and the medium replaced by fresh medium (150 μL) containing 0.5 mg/mL MTT. Three hours later, the MTT formazan product was dissolved in 150 μL DMSO, and absorbance was measured using a multiplate reader (Spectra Count, Packard, Ontario, Canada). Drug effect was quantified as the percentage of control absorbance of the reduced dye at 595 nm. Doxorubicin (0.001-1.06 μM) was used as positive control. Experiments were carried out in triplicate and repeated at least three times.

Lipid peroxidation (TBARS assay). The extent of tested compound-induced lipid peroxidation was determined by the reaction of thiobarbituric acid (TBA) with

malondialdehyde (MDA), a product formed by lipid peroxidation.[52] The assays were performed according to Salgo and Pryor,[53] with minor modifications. Cells were incubated with compound for 24 h, and after lysis with Tris-HCl (15 mM for 1 h). Two milliliters 0.4 mg/mL trichloroacetic acid, 0.25 M HCl were added to the lysate, which was then incubated with 6.7 mg/mL TBA for 15 min at 100 ºC. The mixture was centrifuged at 750 x g for 10 min. As TBA reacts with other products of lipid peroxidation in addition to MDA, results are expressed in terms of thiobarbituric reactive species (TBARS), which are determined by absorbance at 532 nm. Hydrolyzed 1,1,3,3-tetramethoxypropan was used as the standard. The results were normalized by protein content.[54] In order to evaluate the contribution of ROS on lipid peroxidation extent, cells were pre-treated for 24 h with NAC (5 mM), and after they were exposed to tested compound during 24 h. H_2O_2 (10 μM) was used as positive control. All experiments were performed in triplicate in three independent experiments.

Determination of reduced (GSH), oxidized (GSSG) glutathione, and GSG/GSSG ratios. Total glutathione (GSH + GSSG) was determined by spectrophotometer determination of 5-thio-2-nitrobenzoate (TNB), which was produced from DTNB, according to Akerboom and Sies[55] with minor modification. Briefly, cells were exposed with tested compound (5 μM) during 24 h. Then, cells were washed with ice-cold PBS, and resuspended in 0.1 sodium phosphate (5 mM EDTA, pH 8.0), and sonicated to obtain the cell homogenate. An equal volume of 2 M $HClO_4$-4 mM EDTA was added to the cell extract, and the precipitated proteins were sedimented by centrifugation at 8000 x g for 15 min at 4 ºC. The supernatant was neutralized with 2 M KOH, and the insoluble residue was removed by centrifugation under the same conditions. For the

spectrophotometric determination 910 μL of the cell extract supernatant or of the standard glutathione solution, in the same phosphate-EDTA buffer, were mixed with 50 μL of 4 mg/mL NADPH in 0.5% (w/v) $NaHCO_3$, 20 μL of 6 U/mL glutathione reductase in phosphate-EDTA buffer, and 20 μL of 1.5 mg/mL DTNB in 0.5% $NaHCO_3$. The increase in absorbance was measured at 412 nm. The results were normalized by protein content.[54] Total glutathione content was determined as μg/mg protein. For GSSG determination, 4-vinypyridine was added to a final concentration of 0.1% (v/v), and then incubated for 1 h at room temperature. At this concentration, 4-vinypyridine is able to react with all GSH without interfering with GSSG determination. GSH was determined based on the total glutathione and GSSG concentration results. In order to evaluate the contribution of ROS on glutathione modulation content, cells were pre-treated for 24 h with NAC (5 mM), and after they were exposed to tested compound during 24 h. All experiments were performed in triplicate in three independent experiments.

Alkaline comet assay (Single cell gel electrophoresis). The alkaline comet assay was performed as described by Singh et al.[56] with minor modifications,[57] and following the recommendations of the International Workshop on Genotoxicity Test Procedures.[58] At the end of the treatment with **11** (2.5, 5, and 10 μM during 24 h) exposure in the presence or absence of 5 mM NAC (pre-treated for 24 h), cells were washed with ice-cold PBS, detached with 100 μL trypsin (0.15%) and resuspended in complete RPMI medium. Next, 20 μL of cell suspension (~10^6 cells/mL) were mixed with 0.75% low melting point agarose and immediately spread onto a glass microscope slide precoated with a layer of 1% normal melting point agarose. The agarose was allowed to set at 4˚C

for 5 min. The slides were incubated in ice-cold lysis solution (2.5 M NaCl, 10mM Tris, 100mM EDTA, 1% Triton X-100 and 10% DMSO, pH 10.0) at 4˚C for a minimum of 1 h to remove cellular proteins, leaving the DNA as "nucleoids." After the lysis procedure, the slides were placed on a horizontal electrophoresis unit. The unit was filled with fresh buffer (300 mM NaOH and 1mM EDTA, pH>13.0) to cover the slides for 20 min at 4˚C to allow DNA unwinding and expression of alkali-labile sites. Electrophoresis was conducted for 20 min at 25 V and 300 mA (0.86 V/cm). After electrophoresis, the slides were neutralized (0.4 M Tris, pH 7.5), stained with ethidium bromide (20 μg/mL) and analyzed using a fluorescence microscope. All the above steps were conducted under yellow light or in the dark to prevent additional DNA damage. Images of 100 randomly selected cells (50 cells from each of two replicate slides) were analyzed for each concentration of test substance. Cells were scored visually and assigned to one of five classes, according to tail size (from undamaged-0, to maximally damaged-4), and a DNA strand breaks index value was calculated for each sample of cells. DNA strand breaks index thus ranged from 0 (completely undamaged: 100 cells x 0) to 400 (with maximum damage: 100 cells x 4).[59]

Spectral characterization. Spectral characterization of BODIPY-prodrug conjugates. Spectroscopic and quantum yield data were recorded on a Synergy HT spectrophotometer (Biotek). Compounds were dissolved at the indicated concentrations and spectra were recorded at r.t. Spectra are represented as means from at least two independent experiments with n = 3. Quantum yields were calculated by measuring the integrated emission area of the fluorescence spectra and comparing it to the area measured for fluorescein in basic EtOH.

Fluorescence confocal microscopy. PC3 cells were grown in DMEM cell culture media supplemented with 10% FBS, antibiotics (100 U mL^{-1} penicillin and 100 mg mL^{-1} streptomycin) and 2 mM L-glutamine in a humidified atmosphere at 37 °C with 5% CO_2. Cells were plated on glass chamber slides Lab-Tek™ II (Nunc), incubated with compounds **11** or **15** (5 μM) with or without Tracker dyes at 37 °C for 10 min. Cells were imaged in phenol red-free DMEM under a Zeiss LSM 510 META fluorescence confocal microscope equipped with a live cell imaging stage. Fluorescence and brightfield images were acquired using a 40X oil objective. Fluorophores were excited with 488 nm (compound **15**) or 543 nm (Lysotracker Red, Mititarcker Red) lasers. All images were analysed and processed with ImageJ.

Acknowledgements

This research was funded by grants from the Conselho Nacional de Desenvolvimento Científico e Tecnológico (CNPq 305385/2014-3, PVE 401193/2014-4, 477346/2013-8 and Edital Universal MCTI/CNPq Nº 01/2016), FAPEMIG (APQ-02478-14) and Programa Pesquisador Mineiro (PPM-00638-16), INCT-Catálise, CAPES/DAAD 99999.008126/2015-01 and CAPES. M. V. acknowledges the Medical Research Council, the Marie Curie Integration Grant (333847), and the Biotechnology and Biological Sciences Research Council (BB/M025160/1). The authors acknowledge Dr. Bin-Zhi Qian (Univ. Edinburgh) for the supply of PC3 cancer cells for imaging studies.

Notes and References

1. Lombardino JG, Lowe JA. *Nat Rev Drug Discov*. 2004;3:853-862.

2. (a) Meng XY, Zhang HX, Mezei M, Cui M. *Curr Comput Aided Drug Des*. 2011;7:146-157. (b) Moitessier N, Pottel J, Therrien E, Englebienne P, Liu Z, Tomberg A, Corbeil CR. *Acc Chem Res*. 2016;49:1646-1657.

3. Cernak T, Dykstra KD, Tyagarajan S, Vachal P, Krska SW. *Chem Soc Rev*. 2016;45:546-576.

4. (a) Kingston DGI. *J Nat Prod*. 2011;74:496-511. (b) Yraola F, Ventura R, Vendrell M, Colombo A, Fernàndez JC, de la Figuera N, Fernández-Forner D, Royo M, Forns P, Albericio F. *QSAR & Comb Sci*. 2004;23:145-152. (c) Vendrell M, Angulo E, Casadó V, Lluis C, Franco R, Albericio F, Royo M. *J Med Chem*. 2007;50:3062-3069. (d) Vendrell M, Soriano A, Casadó V, Díaz JL, Lavilla R, Canela EI, Lluís C, Franco R, Albericio F, Royo M. *ChemMedChem*. 2009;4:1514-1522.

5. Newman DJ, Cragg GM. *J Nat Prod*. 2016;79:629-661.

6. Brentjens RJ. *Blood*. 2012;119:3872-3873.

7. (a) Rudin M, Weissleder R. *Nat Rev Drug Discov*. 2003;2:123-131. (b) Sittampalam G, Westmore M. *Anal Bioanal Chem*. 2003;377:953-954.

8. (a) Araújo AJ, de Souza AA, da Silva Júnior EN, Marinho-Filho JDB, de Moura MABF, Rocha DD, Vasconcellos MC, Costa CO, Pessoa C, de Moraes MO, Ferreira VF, de Abreu FC, Pinto AV, Montenegro RC, Costa-Lotufo LV, Goulart MOF. *Toxicol in Vitro*. 2012;26:585-594. (b) Park SJ, Yeo HC, Kang NY, Kim H, Lin J, Ha HH, Vendrell M, Lee JS, Chandran Y, Lee DY, Yun SW, Chang YT. *Stem Cell Res*. 2014; 12:730-741.

8. (a) Hillard EA, de Abreu FC, Ferreira DCM, Jaouen G, Goulart MOF, Amatore C. *Chem Commun*. 2008:2612-2628. (b) Parkinson EI, Hergenrother PJ. *Acc Chem Res*. 2015;48:2715-2723. (c) de Paiva YG, Ferreira FR, Silva TL, Labbe E, Buriez O, Amatore C, Goulart MOF. *Curr Top Med Chem*. 2015;15:136-162.

9. (a) Ma J, Lim C, Sacher JR, Houten BV, Qian W, Wipf P. *Bioorg Med Chem Lett*. 2015;25:4828-4833. (b) Inagaki R, Ninomiya M, Tanaka K, Koketsu M. *ChemMedChem*. 2015;10:1413-1423. (c) Ding Q, Zhang Y, Shen Z, Song C, Chang J. *Helv Chim Acta*. 2015;98:128-134.

10. de Castro SL, Emery FS, da Silva Júnior EN. *Eur J Med Chem*. 2013;69:678-700.

11. (a) da Silva Júnior EN, Cavalcanti BC, Guimarães TT, Pinto MCFR, Cabral IO, Pessoa C, Costa-Lotufo LV, de Moraes MO, de Andrade CKZ, dos Santos MR, de Simone CA, Goulart MOF, Pinto AV. *Eur J Med Chem*. 2011;46:399-410. (b) Jardim GAM, Guimarães TT, Pinto MCFR, Cavalcanti BC, de Farias KM, Pessoa C, Gatto CC, Nair DK, Namboothiri INN, da Silva Júnior EN. *Med Chem Commun*. 2015;6:120-130. (c) Vieira AA, Brandão IR, Valença WO, de Simone CA, Cavalcanti BC, Pessoa C, Carneiro TR, Braga AL, da Silva Júnior EN. *Eur J Med Chem*. 2015;101:254-265.

12. da Silva Júnior EN, de Deus CF, Cavalcanti BC, Pessoa C, Costa-Lotufo LV, Montenegro RC, de Moraes MO, Pinto MCFR, de Simone CA, Ferreira VF, Goulart MOF, de Andrade CKZ, Pinto AV. *J Med Chem*. 2010;53:504-508.

13. Lim SM, Jeong Y, Lee S, Im H, Tae HS, Kim BG, Park HD, Park J, Hong S. *J Med Chem*. 2015;58:8491-8502.

14. Cardoso MFC, da Silva IMCB, dos Santos Júnior HM, Rocha DR, Araújo AJ, Pessoa C, de Moraes MO, Lotufo LVC, da Silva FC, Santos WC, Ferreira VF. *J Braz Chem Soc*. 2013;24:12-16.

15. Bonifazi EL, Ríos-Luci C, León LG, Burton G, Padrón JM, Misico RI. *Bioorg Med Chem*. 2010;18:2621-2630.

16. (a) Jiménez-Alonso S, Orellana HC, Estévez-Braun A, Ravelo AG, Pérez-Sacau E, Machín F. *J Med Chem*. 2008;51:6761-6772. (b) Kongkathip N, Kongkathip B, Siripong P, Sangma C, Luangkamin S, Niyomdecha M, Pattanapa S, Piyaviriyagul S, Kongsaeree P. *Bioorg Med Chem*. 2003;11:3179-3191. (c) Netto CD, da Silva AJM, Salustiano EJS, Bacelar TS, Riça IG, Cavalcante MCM, Rumjanek VM, Costa PRR. *Bioorg Med Chem*. 2010;18:1610-1616.

17. Bey EA, Bentle MS, Reinicke KE, Dong Y, Yang CR, Girard L, Minna JD, Bornmann WG, Gao J, Boothman DA. *Proc Natl Acad Sci U.S.A*. 2007;104:11832-11837.

18. Bey EA, Wuerzberger-Davis SM, Pink JJ, Yang CR, Araki S, Reinicke KE, Bentle MS, Dong Y, Cataldo E, Criswell TL, Wagner MW, Li L, Gao J, Boothman DA. *J Cell Physiol*. 2006;209:604-610.

19. Bentle MS, Reinicke KE, Dong Y, Bey EA, Boothman DA. *Cancer Res*. 2007;67:6936-6945.

20. Ohayon S, Refua M, Hendler A, Aharoni A, Brik A. *Angew Chem Int Ed*. 2014;54:599-603.

21. da Cruz EHG, Carvalho PHPR, Corrêa JR, Silva DAC, Diogo EBT, de Souza Filho JD, Cavalcanti BC, Pessoa C, de Oliveira HCB, Guido BC, da Silva Filho DA, Neto BAD, da Silva Júnior EN. *New J Chem*. 2014;38:2569-2580.

22. Shaul P, Frenkel M, Goldstein EB, Mittelman L, Grunwald A, Ebenstein Y, Tsarfaty I, Fridman M. *ACS Med Chem Lett*. 2013;4:323-328.

23. (a) Gontijo TB, de Freitas RR, de Lima GF, de Rezende LCD, Pedrosa LF, Silva TL, Goulart MOF, Cavalcanti BC, Pessoa C, Bruno MP, Corrêa JR, Emery FS, da Silva Júnior EN. *Chem Commun*. 2016;52:13281-13284. (b) Lee JS, Vendrell M, Chang YT. *Curr Opin Chem Biol*. 2011;15:760-767. (c) Vendrell M, Zhai D, Er JC, Chang YT. *Chem Rev*. 2012;112:4391-4420. (d) Kowada T, Maeda H, Kikuchi K. *Chem Soc Rev*. 2015;44:4953-4972.

24. Bahia SBBB, Reis WJ, Jardim GAM, Souto FT, de Simone CA, Gatto CC, Menna-Barreto RFS, de Castro SL, Cavalcanti BC, Pessoa C, Araujo MH, da Silva Júnior EN. *Med Chem Commun*. 2016;7:1555-1563.

25. da Cruz EHG, Silvers MA, Jardim GAM, Resende JM, Cavalcanti BC, Bomfim IS, Pessoa C, de Simone CA, Botteselle GV, Braga AL, Nair DK, Namboothiri INN, Boothman DA, da Silva Júnior EN. *Eur J Med Chem*. 2016;122:1-16.

26. (a) Kolb HC, Sharpless KB. *Drug Discovery Today*. 2003;8:1128-1137. (b) Kolb HC, Finn MG, Sharpless KB. *Angew Chem Int Ed*. 2001;40:2004-2021. (c) Tornøe CW, Christensen C, Meldal M. *J Org Chem*. 2002;67:3057-3064. (d) Rostovtsev VV, Green LG, Fokin VV, Sharpless KB. *Angew Chem Int Ed*. 2002;41:2596-2599. (e) Meldal M, Tornøe CW. *Chem Rev*. 2008;108:2952-3015.

27. (a) Lee JS, Kang NY, Kim YK, Samanta A, Feng S, Kim HK, Vendrell M, Park JH, Chang YT. *J Am Chem Soc*. 2009;131:10077-10082. (b) Vázquez-Romero A, Kielland N, Arévalo MJ, Preciado S, Mellanby RJ, Feng Y, Lavilla R, Vendrell M. *J Am Chem Soc*. 2013;135:16018-16021. (c) Rezende LCD, Vaidergorn MM, Moraes JCB, Emery FS. *J Fluoresc*. 2014;24:257-266. (d) Vendrell M, Krishna GG, Ghosh KK, Zhai D, Lee JS, Zhu Q, Yau YH, Shochat SG, Kim H, Chung J, Chang YT. *Chem Commun*. 2011;47:8424-8426. (e) Er JC, Vendrell M, Tang MK, Zhai D, Chang YT. *ACS Comb Sci*. 2013;15:452-457. (f) Vázquez-Romero A, Kielland N, Arévalo MJ, Preciado S, Mellanby RJ, Feng Y, Lavilla R, Vendrell M. *J Am Chem Soc*. 2013;135:16018-16021. (g) Mendive-Tapia L, Zhao C, Akram AR, Preciado S, Albericio F, Lee M, Serrels A, Kielland N, Read ND, Lavilla R, Vendrell M. *Nat Commun*. 2016;7:10940.

28. For review articles see: (a) Bessette A, Hanan GS. *Chem Soc Rev*. 2014;43:3342-3405. (b) Boens N, Leen V, Dehaen W. *Chem Soc Rev*. 2012;41:1130-1172. (c) Loudet A, Burgess K. *Chem Rev*. 2007;107:4891-4932. (d) Fernandez A, Vendrell M. *Chem Soc Rev* 2016;45:1182-1196. (e) De Moliner F, Kielland N, Lavilla R, Vendrell M. *Angew Chem Int Ed* 2017; 56:3758–3769.

29. (a) Rohand T, Dolusic E, Ngo TH, Maes W, Dehaen W. *Arkivoc*. 2007;10:307-324. (b) Rohand T, Baruah M, Qin W, Boens N, Dehaen W. *Chem Commun*. 2006;266-268.

30. da Silva Júnior EN, de Souza MCBV, Fernandes MC, Menna-Barreto RFS, Pinto MCFR, Lopes FA, de Simone CA, Andrade CKZ, Pinto AV, Ferreira VF, de Castro SL. *Bioorg Med Chem*. 2008;16:5030-5038.

31. Guimarães TT, Pinto MCFR, Lanza JS, Melo MN, do Monte-Neto RL, de Melo IMM, Diogo EBT, Ferreira VF, Camara CA, Valença WO, de Oliveira RN, Frézard F, da Silva Júnior EN. *Eur J Med Chem*. 2013;63:523-530.

32. da Silva Júnior EN, Menna-Barreto RFS, Pinto MCFR, Silva RSF, Teixeira DV, de Souza MCBV, de Simone CA, de Castro SL, Ferreira VF, Pinto AV. *Eur J Med Chem*. 2008;43:1774-1780.

33. Fieser LF, Fieser M. *J Am Chem Soc*. 1948;70:3215-3222.

34. Pérez-Sacau E, Díaz-Peñate RG, Estévez-Braun A, Ravelo AG, García-Castellano JM, Pardo L, Campillo M. *J Med Chem*. 2007;50:696-706.

35. da Cruz EHG, Hussene CMB, Dias GG, Diogo EBT, de Melo IMM, Rodrigues BL, da Silva MG, Valença WO, Camara CA, de Oliveira RN, de Paiva YG, Goulart MOF, Cavalcanti BC, Pessoa C, da Silva Júnior EN. *Bioorg Med Chem*. 2014;22:1608-1619.

36. Viegas Júnior C, Danuello A, Bolzani VS, Barreiro EJ, Fraga CAM. *Curr Med Chem*. 2007;14:1829-1852.

37. (a) Monks TJ, Hanzlik RP, Cohen GM, Ross D, Graham DG. *Toxicol Appl Pharmacol*. 1992;112:2-16. (b) Portela MPM, Stoppani AOM. *Biochem Pharmacol*. 1996;51:275-283.

38. Abreu FC, Goulart MOF, Brett AMO. *Electroanalysis*. 2002;14:29-34.

39. Bolton JL, Trush MA, Penning TM, Dryhurst G, Monks TJ. *Chem Res Toxicol*. 2000;13:135-160.

40. Zafarullah M, Li WQ, Sylvester J, Ahmad M. *Cell Mol Life Sci*. 2003;60:6-20.

41. Mikhed Y, Daiber A, Steven S. *Int J Mol Sci*. 2015;16:15918-15953.

42. O'Brien PJ. *Chem Biol Interact*. 1991;80:1-41.

43. (a) Gros L, Saparbaev MK, Laval J. *Oncogene*. 2002;21:8905-8925. (b) Feng D, Huang H, Yang Y, Yan T, Jin Y, Cheng X, Cui L. *Mutat Res Genet Toxicol Environ Mutagen.* 2015;792:35-45.

44. (a) Begleiter A, Blair GW. *Cancer Res.* 1984;44:78-82. b) Walles SA. *Cancer Lett*. 1992;63:47-52. (c) Saibu M, Sagar S, Green I, Ameer F, Meyer M. *Anticancer Res.* 2014;34:4077-4086.

45. (a) Speit G, Schütz P, Bonzheim I, Trenz K, Hoffmann H. *Toxicol Lett*. 2004;146:151-158. (b) Kushwaha S, Vikram A, Trivedi PP, Jena GB. *Mutat Res*. 2011;726:242-250.

46. (a) Meister A. *Pharmacol Ther*. 1991;51:155-194. (b) Er JC, Tang MK, Chia CG, Liew H, Vendrell M, Chang YT. *Chem Sci*. 2013;4:2168-2176. (c) Zhang L, Er JC, Jiang H, Li X, Luo Z, Ramezani T, Feng Y, Tang MK, Chang YT, Vendrell M. *Chem Commun*. 2016;52:9093-9096.

47. Patil NG, Basutkar NB, Ambade AV. *Chem Commun*. 2015;51:17708-17711.

48. (a) Zhang C, Zhao J, Wu S, Wang Z, Wu W, Ma J, Guo S, Huang L. *J Am Chem Soc*. 2013;135:10566-10578. (b) Magde D, Wong R, Seybold PG. *Photochem Photobiol*. 2007;75:327-334.

49. Sukhai MA, Prabha S, Hurren R, Rutledge AC, Lee AY, Sriskanthadevan S, Sun H, Wang X, Skrtic M, Seneviratne A, Cusimano M, Jhas B, Gronda M, MacLean N, Cho EE, Spagnuolo PA, Sharmeen S, Gebbia M, Urbanus M, Eppert K,

Dissanayake D, Jonet A, Dassonville-Klimpt A, Li X, Datti A, Ohashi PS, Wrana J, Rogers I, Sonnet P, Ellis WY, Corey SJ, Eaves C, Minden MD, Wang JCY, Dick JE, Nislow C, Giaever G, Schimmer AD. *J Clin Invest*. 2012;123:315-328.

50. Baglole C, Bushinsky SM, Garcia TM, Kode A, Rahman I, Sime PJ, Phipps RP. *Am. J. Physiol. Lung Cell Mol. Physiol*. 2006;291:19-29.

51. Draper HH, Hadley M. *Methods Enzymol*. 1990;186:421-431.

52. Salgo MG, Pryor WA. *Arch Biochem Biophys*. 1996;333:482-488.

53. Lowry OH, Rosebrough NJ, Farr AL, Randall RJ. *J Biol Chem*. 1951;193:265-275.

54. Akerboom TP, Sies H. *Methods Enzymol*. 1981;77:373-382.

55. Singh NP, McCoy MT, Tice RR, Schneider EL. *Exp Cell Res*. 1988;175:184-191.

56. Hartmann A, Speit G. *Toxicol Lett*. 1997;90:183-188.

57. Tice RR, Agurell E, Anderson D, Burlinson B, Hartmann A, Kobayashi H, Miyamae Y, Rojas E, Ryu JC, Sasaki YF. *Environ Mol Mutagen*. 2000;35:206-221.

58. Cavalcanti BC, Ferreira JRO, Moura DJ, Rosa RM, Furtado GV, Burbano RR, Silveira ER, Lima MAS, Camara CAG, Saffi J, Henriques JAP, Rao VSN, Costa-Lotufo LV, Moraes MO, Pessoa C. *Mutat Res*. 2010;701:153-163.

Supplementary Material

Click here to download Supplementary Material: Supplementary Information - 04.06.2017.docx